ilmedia

TECHNISCHE UNIVERSITÄT
ILMENAU

Asghar, Muhammad Talal; Frank, Thomas; Schwierz, Frank

Failure analysis of wire bonding on strain gauge contact pads using FIB, SEM, and elemental mapping

Original published in:	Engineering proceedings. - Basel : MDPI. - 6 (2021), 1, art. 53, 4 pp.
Original published:	2021-05-17
ISSN:	2673-4591
DOI:	10.3390/I3S2021Dresden-10142
[*Visited:*	2022-03-03]

This work is licensed under a Creative Commons Attribution 4.0 International license. To view a copy of this license, visit https://creativecommons.org/licenses/by/4.0/

TU Ilmenau | Universitätsbibliothek | ilmedia, 2022
http://www.tu-ilmenau.de/ilmedia

engineering proceedings

MDPI

Proceeding Paper

Failure Analysis of Wire Bonding on Strain Gauge Contact Pads Using FIB, SEM, and Elemental Mapping †

Muhammad Talal Asghar [1,*], Thomas Frank [2] and Frank Schwierz [1]

1 Institut für Mikro- und Nanoelektronik, Technische Universität Ilmenau, PF 100565, 98684 Ilmenau, Germany; frank.schwierz@tu-ilmenau.de
2 CiS Forschungsinstitut für Mikrosensorik GmbH Konrad-Zuse-Straße 14, 99099 Erfurt, Germany; tfrank@cismst.de
* Correspondence: muhammad-talal.asghar@tu-ilmenau.de

† Presented at the 8th International Symposium on Sensor Science, 17–28 May 2021; Available online: https://i3s2021dresden.sciforum.net/.

Abstract: Stacks consisting of titanium, platinum, and gold layers constitute a popular metallization system for the bond pads of semiconductor chips. Wire bonding on such layer stacks at different temperatures has extensively been investigated in the past. However, reliable information on the bondability of this metallization system after a high-temperature sintering process is still missing. When performing wire bonding after pressure sintering (at, e.g., 875 °C), bonding failures may occur that must be identified and analyzed. In the present study, a focused ion beam (FIB), scanning electron microscopy (SEM), and elemental mapping are utilized to characterize the root cause of failure. As a probable root cause, the infusion of metallization layers is found which causes an agglomerate formation at the interface of approximately 2 µm height difference on strain gauge contact pads and possibly an inhomogeneous mixing of layers as a consequence of the high-temperature sintering process. Potential treatment to tackle this agglomeration with the removal of the above-mentioned height difference during the process of contact pad structuring and alternative electrical interconnect methodologies are hereby suggested in this paper.

Keywords: wire bonding; FIB; SEM; metallization system; elemental mapping; sintering

Citation: Asghar, M.T.; Frank, T.; Schwierz, F. Failure Analysis of Wire Bonding on Strain Gauge Contact Pads Using FIB, SEM, and Elemental Mapping. *Eng. Proc.* **2021**, *6*, 53. https://doi.org/10.3390/I3S2021Dresden-10142

Academic Editors: Gianaurelio Cuniberti and Larysa Baraban

Published: 17 May 2021

Publisher's Note: MDPI stays neutral with regard to jurisdictional claims in published maps and institutional affiliations.

Copyright: © 2021 by the authors. Licensee MDPI, Basel, Switzerland. This article is an open access article distributed under the terms and conditions of the Creative Commons Attribution (CC BY) license (https://creativecommons.org/licenses/by/4.0/).

1. Introduction

Traditional mechanical treatment of samples such as grinding and polishing for subsequent structure analysis results in deformations and artifacts that make the visualization of the material structure difficult or even impossible [1,2]. Focused ion beam (FIB) tools are a popular alternative for analysis. Three functions are employed when using FIB which are partial etching, partial metal deposition, and scanning ion/electron microscopy (SEM). Partial etching by FIB can be used for cross sectioning on chip contact pads and scanning ion/electron microscopy can be included in in situ observations as suggested by Kaito et al [3] and applied by Nikawa et al. [4]. In the present study, FIB, SEM, and elemental mapping are used for the failure analysis of wire bonding on strain gauge contact pads on a cross section of almost 10 μm^2.

The 500 µm × 500 µm × 15 µm strain gauge with five contact pads is realized on silicon on insulator. Four wire-bondable contact pads are placed at the corner edges while the fifth pad is located on the insulator between two corner edge contact pads. The structure of the wire-bondable pads consisting of Ti/Pt/Au stacks is illustrated in Figure 1a. The strain gauge itself is completely integrated within ceramic by pressure sintering at 875 °C.

Almost 100% failure of Au and Al wire bonding was observed on the wire-bondable corner contact pads with a non-adhesive behavior of ball and wedge bonds. Varying the bonding parameters such as ultrasonic time, power, and bond force did not yield sufficient bond strength to stick. Both optical and SEM inspections showed no obvious barrier at the

surface of the contact pads during the bonding process. Therefore, the bonding process itself was excluded as a primary factor, and the contact pads of the strain gauge were presumed of being the reason for failure.

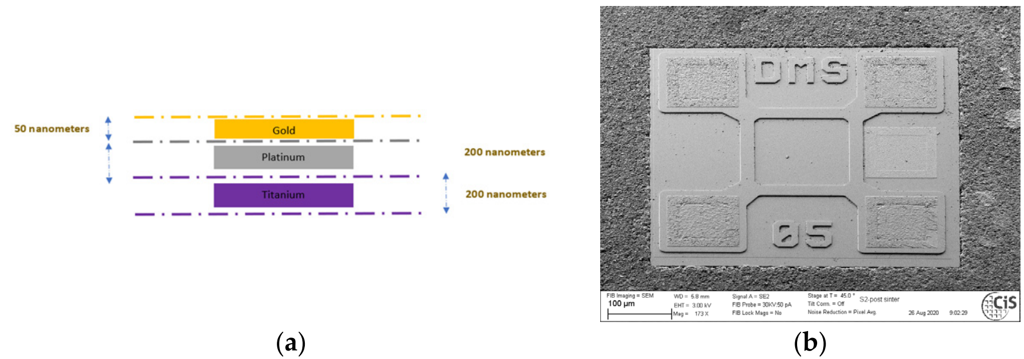

(**a**) (**b**)

Figure 1. (**a**) Metallization stacks of the contact pads at corner edges and (**b**) strain gauge integrated within ceramic.

2. Method and Materials

For the investigation of the underlying cause of the failure, we began the SEM and EDX analysis in combination with the elemental mapping. Laser microscope profilometry using a Keyence 3D confocal microscope (model VK–X 200) has been performed in order to observe the surface topology of the contact pads.

2.1. Contact Pads at Corner Edges

The corner contact pads have been structured in a way that the corner edges have a predefined height difference of 1.932 µm, as illustrated in Figure 2a. This height difference is probably due to the various etching steps for contact pads structuring, which is not straightforward to control.

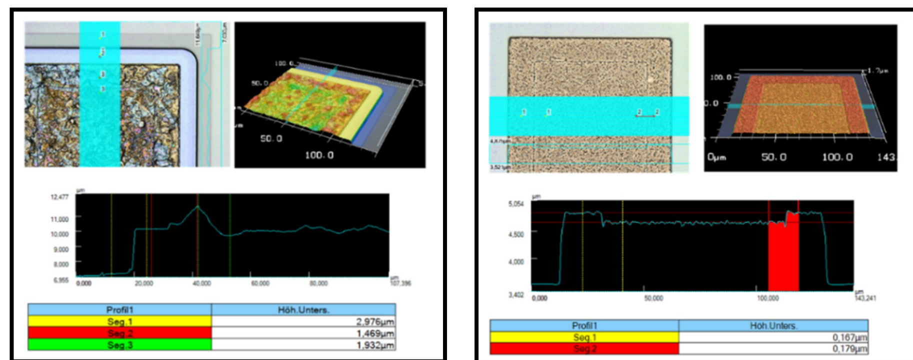

Figure 2. (**a**) Laser profilometry on corner contact pads and (**b**) laser profilometry on the center contact pad.

2.2. Contact Pads on Insulator

Laser profilometry yielded a height difference of 0.179 µm for the center contact pad on insulator. This is insignificant compared to the height difference of the corner contact pads. Therefore, we investigated this corner pad height difference at the interface, considering the earlier mentioned fact that there was no apparent sign of any obvious barrier or oxide formation at the surface of contact pads.

2.3. FIB Cross-Sectioning and SEM/EDX Analysis

To study the interface height difference, a cross sectioning was performed on a 10 μm^2 area on both contact pads, as illustrated in Figure 3. Since it is critical to perform the cross

sectioning by mechanical grinding and polishing (pads will be damaged or peeled during the process), a precise cross sectioning using FIB is performed. Because of the conductivity of the Au on top of the pad, charging effect during the FIB process could be avoided without dispensing conductive material [5]. A coarse chemically enhanced etching with fine milling was performed using 2.0 KeV Ar+ ion beam milling with a IM 4000 system. Finally, the cross section was fine-polished using a low current [6].

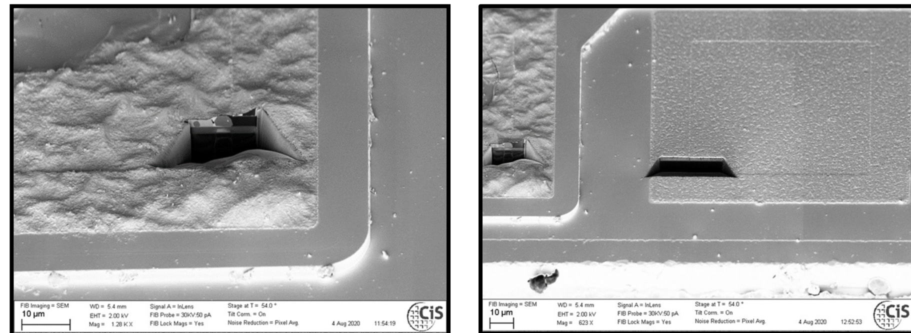

Figure 3. (**a**) FIB cross section at corner contact pad and (**b**) FIB cross section at the center contact pad.

2.4. Combined EDX Analysis

Combining a SEM image and EDX elemental mapping provides a unique analytical perspective for determining the exact composition. Cross-sectioned bond pads were analysed by a Hitachi S—4100 setup, and elemental mapping was conducted at 0.5–3.5 KeV to accurately determine the composition at the focussed SEM image. Four corner pads were studied at a total of sixteen locations by cross sectioning right at the height difference interface.

3. Results and Discussions

For the corner contact pads, at the intersection of 1.932 µm height difference a metallic alloy agglomerate formation was observed as illustrated in Figure 4. It appears that the high temperature sintering at 875 °C forces Ti, Pt, and Au to move at the interface leading to an agglomerate. This alloy formation leads to an altering pad morphology, which ultimately adds to the surface roughness and may affect the wire bond adhesiveness [7].

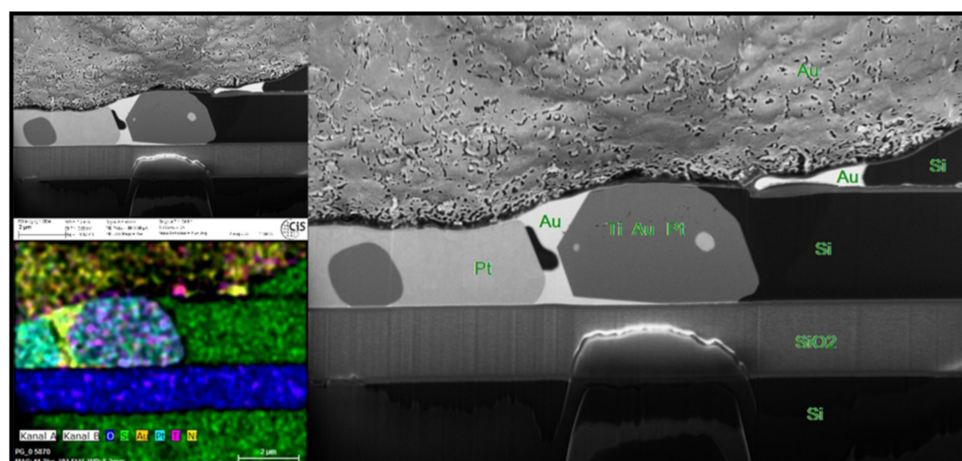

Figure 4. Agglomerate formation on edge contact pads at the interface.

A significantly different situation is observed for the contact pad on insulator. Here, the three metal layers are segregated in between each other, and a more uniform metallization is realized even after firing at high temperature, as illustrated in Figure 5.

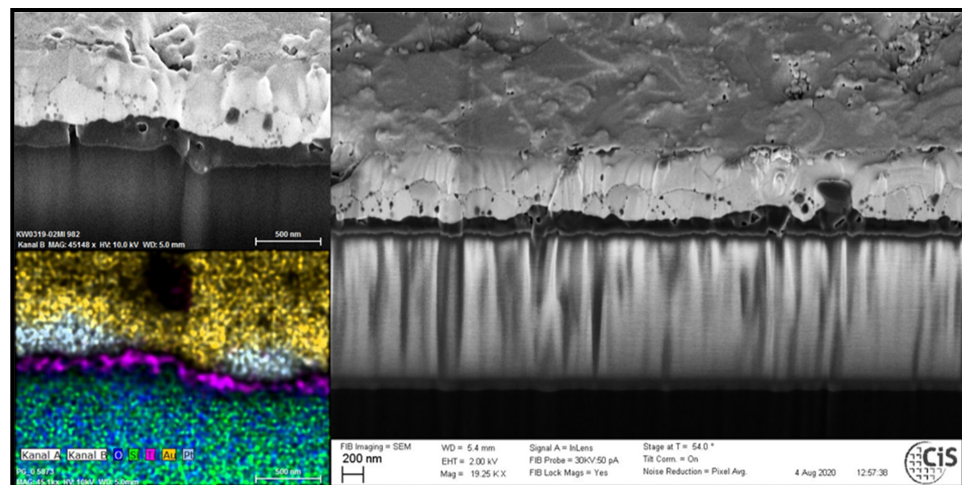

Figure 5. Segregated metallization layers on contact pad on insulator.

4. Conclusions

FIB, SEM, and EDX analysis showed that the likely mechanism for Au and Al wire bond failure problem could be the metallic alloy agglomerate formation underneath the contact pads due to infusion. To confirm the failure mechanism, further experimentation is deemed necessary. An alternative to overcoming this problem can be to make these metallization layers flatter during structuring or to add an additional Au metal layer at the top in order to suppress the negative impact of agglomerate formation at bottom. Possibly screen printing can be investigated as alternative electrical interconnect methodology.

Author Contributions: Experiments, writing—original draft preparation, M.T.A.; conceptualization, supervision, writing—review and editing, T.F.; writing—review and editing, supervision, F.S. All authors have read and agreed to the published version of the manuscript.

Funding: This research activity received no external funding.

Conflicts of Interest: The authors declare no conflict of interest.

References

1. Yang, J.; Odén, M.; Johansson-Jõesaar, M.P.; Llanes, L. Grinding effects on surface integrity and mechanical strength of WC-Co cemented carbides. *Procedia CIRP* **2014**, *13*, 257–263. [CrossRef]
2. Perry, A.J.; Geist, D.E.; Narasimhan, K.; Treglio, J.R. On the state of stress in the surface of ground cemented carbide before and after metal ion implantation. *Surf. Coat. Technol.* **1996**, *86*, 364–371. [CrossRef]
3. Kaito, T.; Adachi, T. Focused ion beam system for IC development and its applications. In Proceedings of the 1st Micro Process Conference, Tokyo, Japan, July 1988; p. 142.
4. Nikawa, M.M.K.; Nasu, K. New applications of focussed ion beam technique to failure analysis and process monitoring of VLSI. In Proceedings of the 27th Annual Proceedings, International Reliability Physics Symposium, Phoenix, AZ, USA, 11−13 April 1989; p. 43. [CrossRef]
5. Stevens-Kalceff, M.A.; Rubanov, S.; Munroe, P.R. Localized Charging Effects Resulting from Focused Ion Beam Processing of Non-Conductive Materials. *MRS Online Proc. Libr.* **2003**, *792*, 74–79. [CrossRef]
6. Zhao, S.P.; Hua, Y.N.; Goh, G.P.; Guo, Z.R.; Chau, K.W. Contamination analyses of Al bond pads using FIB/SEM/EDX. In *the Proceedings of the 1997 6th International Symposium on the Physical and Failure Analysis of Integrated Circuits, Singapore, 25−25 July 1997*; pp. 254–259. [CrossRef]
7. Kokini, K.; Sheets, B.E. Thermal Stresses Under Engine Heat Flux—Part 2: Thin Metallic Films on Ceramic Coatings. *J. Energy Resour. Technol.* **1992**, *114*, 298–308. [CrossRef]